Simulation of forming of paperboard packaging using LS-DYNA

Mikael Schill [1], Johan Tryding [2], Jesper Karlsson [3]

[1] Dynamore Nordic, Linköping, Sweden
[2] Tetra Pak, Lund, Sweden
[3] Dynamore Nordic, Gothenburg, Sweden

1 Introduction

Paperboard is a widely used material for packaging of food and beverage. Since the package contains eatables, the container needs to be aseptic. This means e.g. that the paperboard may not contain in-plane surface cracks that could jeopardize the structural integrity of the container. The cracks could form during the manufacturing and filling of the container.

To be able to form the paperboard into a container, the paperboard has to be folded. To accommodate for the folding, the process is preceded by a creasing process stage. The purpose of the creasing stage is to notch the paperboard and weaken the fiber structure, see Fig. 1. This will enable further delamination and a predetermined direction for the fold.

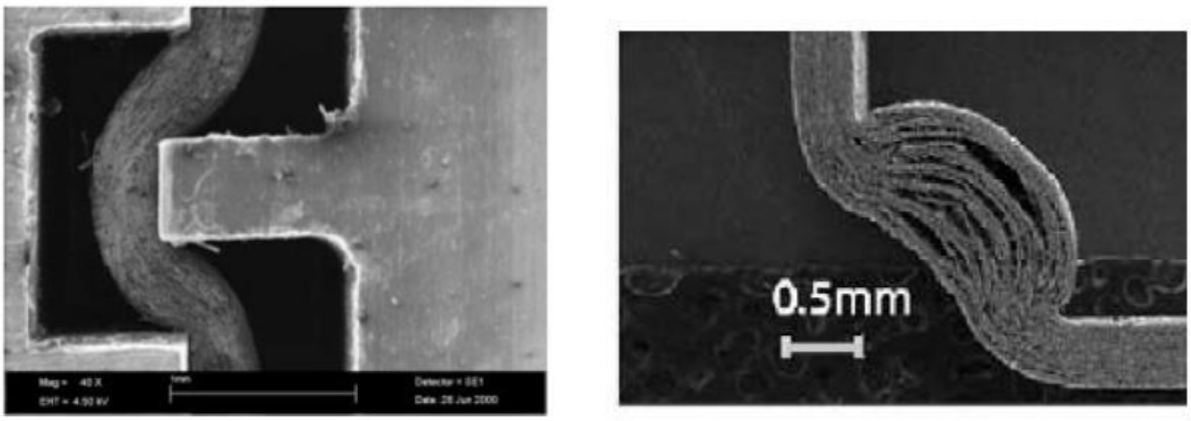

Fig. 1: Creasing of paperboard (left), from Dunn [1] and folding (right) from Nagasawa et al. [2].

2 Paperboard properties

Paperboard consists mainly of cellulose fibers. Due to its fibrous structure, the directions and bonding of the fibers will have a major influence on the paperboard properties. Due to the manufacturing process an orthotropic material is typically produced where the properties are defined in Machine (MD), Cross (CD) and thickness (ZD) directions, see Fig. 2.

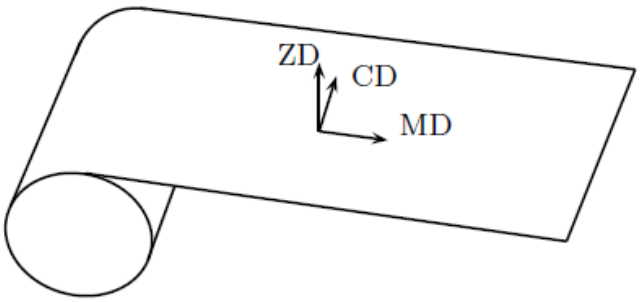

Fig. 2: Illustration of the paperboard orthotropic directions, from Borgqvist [3].

The paperboard can consist of a single ply or multiple plies of different thicknesses and properties. Also, the paperboard can be joined with layers of aluminum foil and/or polyethylene as liquid and light barriers. More details on material testing of paperboard and paperboard properties can be found in e.g. Tryding [4], Mäkelä et al. [5] and Nygårds [6].

2.1 In plane properties

The in-plane properties are typically identified through simple tensile tests in MD, CD and 45 degree directions. The tests are performed for each ply if applicable, see Fig. 3. The test shows a highly anisotropic material, as expected. Also, there is a big difference between the different plies. It is also possible to classify the deformation into an elastic and a plastic region.

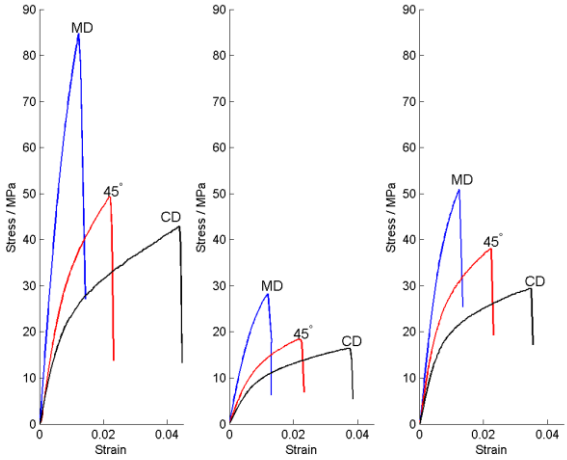

Fig. 3: Typical paperboard tensile properties of different plys and directions (lower, mid and upper), from Nygårds [6].

The properties in compression are determined by using a custom made testing equipment that uses static compression in the ZD to avoid out of plane buckling. The properties are linear up to the maximum point where it is assumed that out of plane effects are dominant, see Fig. 4.

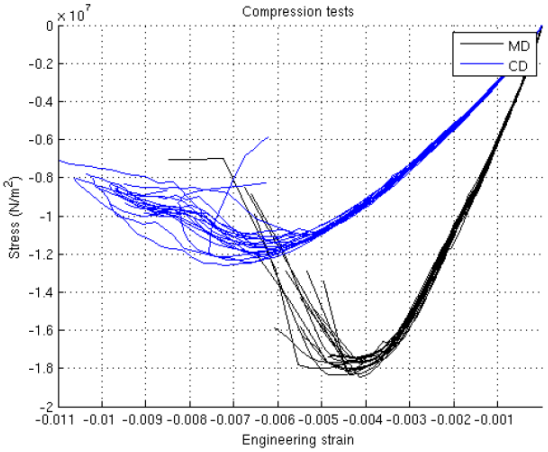

Fig. 4: Typical paperboard in-plane compressive properties in MD and CD directions, from Lindström [7].

2.2 Out of plane properties

In out of plane tension, paperboard shows a linear behavior up to the point of delamination, see Fig. 5 (a). In out of plane compression, the material is non-linear elastic-plastic, see Fig. 5 (b).

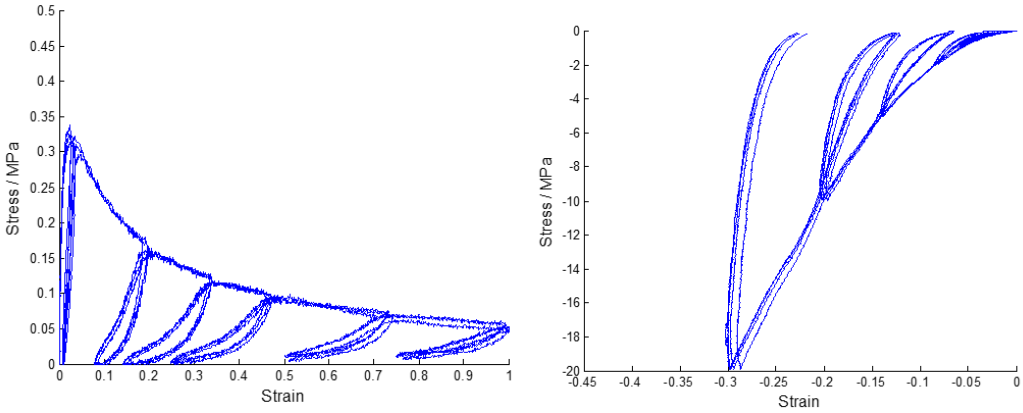

Fig. 5: Typcial out of plane tension (a) and compression behaviour of paperboard, from Nygårds [6].

In out of plane shear, the material shows a dependency on the ZD compressive stress, where the shear strength increases with increasing ZD stress, see Fig. 6.

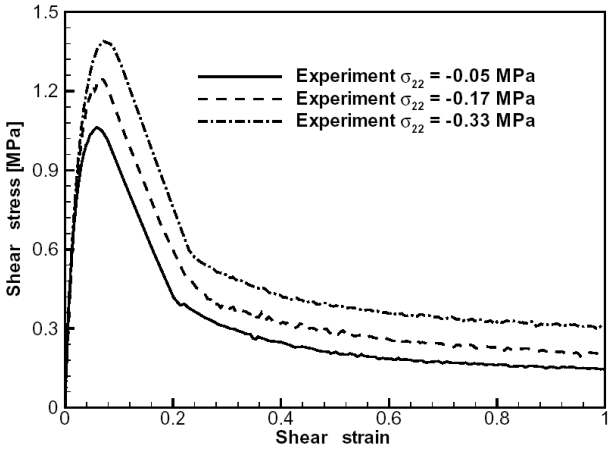

Fig. 6: Typical out of plane shear behaviour and ZD stress dependency, from Stenberg [8].

From figures 5 and 6 it is evident that the out of plane tension and shear behavior shows a softening behavior. This is due to delamination of the paperboard. To accommodate for this, a cohesive model will be used. This is further described in Section 4.2.

3 *MAT_PAPER

The paper material model based on Xia [9] and Nygårds et al. [10] is implemented in LS-DYNA. The material model is denoted *MAT_PAPER and is material type 274. The model has a solid element version which is hyperelastic-plastic, and a shell element version which is hypoelastic-plastic. In the following, the solid (3D) element version is described and the shell element specifics are described in Section 3.3. The implementation is based on an assumption that the in plane model and the out of plane models can be uncoupled, thus solved separately.

3.1 In plane elasticity and plasticity

The in plane and out of plane elasticity is modeled as orthotropic where the 2nd Piola-Kirchoff stress is related to the elastic Green strain through

$$\mathbf{S} = \mathbf{C}\mathbf{E}_\mathbf{e} \tag{1}$$

where $\mathbf{E}_\mathbf{e}$is the Green strain and $\mathbf{C}$ is the constitutive matrix. Using Voigt notation, its inverse can be written as

$$\mathbf{C}^{-1} = \begin{bmatrix} \frac{1}{E_1} & -\frac{\nu_{21}}{E_2} & -\frac{\nu_{31}}{E_3} & & & \\ -\frac{\nu_{12}}{E_1} & \frac{1}{E_2} & -\frac{\nu_{32}}{E_3} & & & \\ -\frac{\nu_{13}}{E_1} & -\frac{\nu_{23}}{E_2} & \frac{1}{E_3} & & & \\ & & & \frac{1}{G_{12}} & & \\ & & & & \frac{1}{G_{23}} & \\ & & & & & \frac{1}{G_{13}} \end{bmatrix} \tag{2}$$

The in plane yield surface is constructed by six different yield planes. The yield planes are:

1. Tension in MD
2. Tension in CD
3. Positive in plane shear
4. Compression in MD
5. Compression in CD
6. Negative in plane shear.

The yield planes are combined to an in plane yield surface using

$$f = \sum_{i=1}^{6} \left[\frac{S{:}N_i}{q_i(\varepsilon_p^f)} \right]^{2k} - 1 \leq 0 \tag{3}$$

where N_i is the normal direction to the respective yield planes, *2k* is a positive integer, $q_i$is the respective hardening and $\varepsilon_p^f$is the inplane plastic strain. The respective directions of the yield planes are given as

$$N_1 = \begin{bmatrix} \frac{1}{\sqrt{1+\nu_{1p}^2}} & -\frac{\nu_{1p}}{\sqrt{1+\nu_{1p}^2}} & 0 & 0 & 0 & 0 \end{bmatrix}^T \tag{4}$$

$$N_2 = \begin{bmatrix} -\frac{\nu_{2p}}{\sqrt{1+\nu_{2p}^2}} & \frac{1}{\sqrt{1+\nu_{2p}^2}} & 0 & 0 & 0 & 0 \end{bmatrix}^T \tag{5}$$

$$N_3 = \begin{bmatrix} 0 & 0 & 0 & \sqrt{2} & 0 & 0 & 0 \end{bmatrix}^T \tag{6}$$

$$N_4 = -\begin{bmatrix} \frac{1}{\sqrt{1+\nu_{4p}^2}} & -\frac{\nu_{4p}}{\sqrt{1+\nu_{4p}^2}} & 0 & 0 & 0 & 0 \end{bmatrix}^T \tag{7}$$

$$N_5 = -\begin{bmatrix} -\frac{\nu_{5p}}{\sqrt{1+\nu_{5p}^2}} & \frac{1}{\sqrt{1+\nu_{5p}^2}} & 0 & 0 & 0 & 0 \end{bmatrix}^T \tag{8}$$

$$N_6 = -N_3 \tag{9}$$

again, using Voigt notation. The parameters $\upsilon_{ip}$are the plastic Posson's ratios. The hardening, q_i, can be given as an analytic expression

$$q_i\left(\varepsilon_p^f\right) = S_i^0 + A_i^0 \tanh\left(B_i^0 \varepsilon_p^f\right) + C_i^0 \varepsilon_p^f \tag{10}$$

where $S_i^0, A_i^0, B_i^0$and $C_i^0$are hardening constants. If $S_i^0$is input as negative, its absolute value is referring to a load curve.

A typical initial yield surface and corresponding failure surface is shown in Fig. 7.

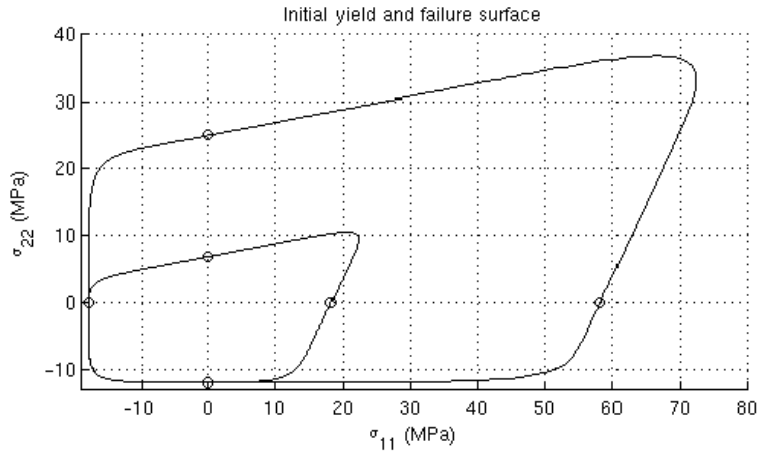

Fig. 7: Typical initial and failure in plane yield surface of paperboard, from Lindström [7].

3.2 Out of plane elasticity and plasticity

In out of plane compression, the stress is modified as

$$S_{33} = C_{31}E_{11}^e + C_{32}E_{22}^e + E_3^c\left[1 - e^{-C_c E_{33}^e}\right] \tag{11}$$

to model a nonlinear elastic compression behavior using material constants E_3^c and C_c. In out of plane tension, the material model is always elastic since the cohesive model described below will describe the delamination. However, in out of plane compression, the yield surface is given as

$$g = \frac{-S_{33}}{A_\sigma + B_\sigma e^{-C_\sigma \varepsilon_p^g}} - 1 \leq 0 \tag{12}$$

where A_σ, B_σ and C_σ are hardening constants and $\varepsilon_p^g$is the out of plane compression plastic strain. The transverse shear yield surface is given as

$$h = \frac{\sqrt{S_{13}^2 + S_{23}^2}}{\tau_0 + [A_\tau - S_{33}B_\tau]\varepsilon_p^h} - 1 \leq 0 \tag{13}$$

where τ_0, A_τ and B_τ are hardening parameters and where the latter control the influence from the out of plane compression stress. The transverse shear plastic strain is denoted ε_p^h

3.3 Shell element specifics

A hypoelastic approach is used for shell elements and the rate of deformation is split into an elastic and a plastic part through

$$\mathbf{D} = \mathbf{D_e} + \mathbf{D_p} \tag{14}$$

and the rate of the Cauchy stress is given by

$$\boldsymbol{\sigma} = \overset{\cdot}{\mathbf{C}}\mathbf{D_e} \tag{15}$$

Compared to equation (11), the out of plane compression stress is modified as

$$\dot{\sigma}_{33} = C_{31}D_{11}^e + C_{32}D_{22}^e + D_{33}^e E_3^c e^{-C_c \varepsilon_e^{33}} \tag{16}$$

For shells, only the in plane yield surface (3) and the transverse shear yield surface (13) are present.

4 Paperboard modeling

Depending on the application and/or region of the container, different modeling techniques has to be used. If the overall stiffness of the paperboard is the primary concern, a shell element mesh is a valid

choice. However, if delamination is of interest e.g. in the vicinity of a creasing line it is necessary to use cohesive elements between layers of either shells or solid elements.

4.1 In-plane properties

If only the in plane properties are of interest, a shell approach is a sufficient choice of element. In this case, the stresses in the ZD direction will be zero and the material has no ability to delaminate. Another choice would be to use a thick shell element. However, the thickness of the element will then affect the critical timestep. The resemblance with composites modeling is obvious and for layered plies it is certainly possible to use the ***PART_COMPOSITE** keyword. By this the user is able to stack various paperboard materials with various thicknesses to form a multiply laminate.

4.2 Out of plane delamination

To enable for the paperboard to delaminate in ZD tension and out of plane shear, cohesive layers are added, see Fig. 8. The number of cohesive layers are not necessarily determined by the number of plies. Instead it is determined by experience and experimental reference. The constitutive equations for cohesive elements are formulated by tractions and separations rather than stresses and strains. In this work the *MAT_COHESIVE_GENERAL material model has been used and the fracture energies and maximum tractions in normal and shear directions are determined from Nygårds et al. [10].

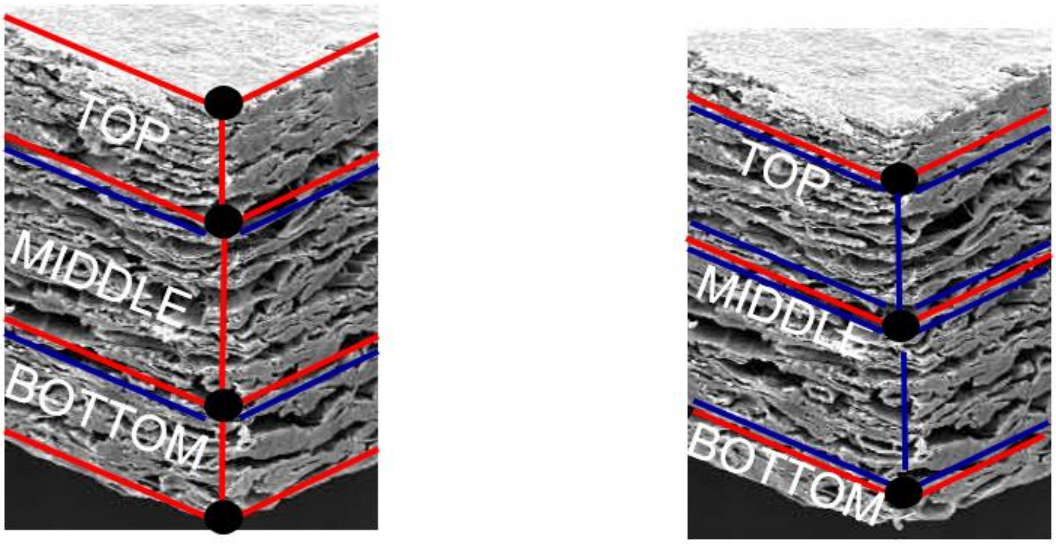

Fig. 8: Through thickness modeling with cohesive layers for delamination using solid elements (left) and shell elements (right). Finite elements are showed as red and cohesive elements as blue.

If the cohesive elements are used together with solid elements, the ZD compression response is determined by the paper material model and the penetration stiffness of the cohesive material should be large enough to avoid penetration of the different plies. The cohesive elements will then be modeled with zero thickness. However, if shell elements are used to model the different plies, the cohesive elements will have the thickness of the distances between the shell elements. In this case, the cohesive element type 20 have be used that enables a consistent application of the forces and moments using the offset between the shell surfaces. It should however be mentioned that by using shell elements and cohesive elements, the ZD compression will be determined by the penetration stiffness and the shear traction will not be dependent on the ZD compression stress. To enable this, a more suitable cohesive material model has to be implemented.

5 Simulations

5.1 Bending

The in plane properties of the paperboard can be measured using a bending test, see Fig. 9. The paperboard is clamped at one end and rotated. A load cell measures the counteracting force from the torque. By varying the distance between the load cell and the clamping point, different bending radii can be generated.

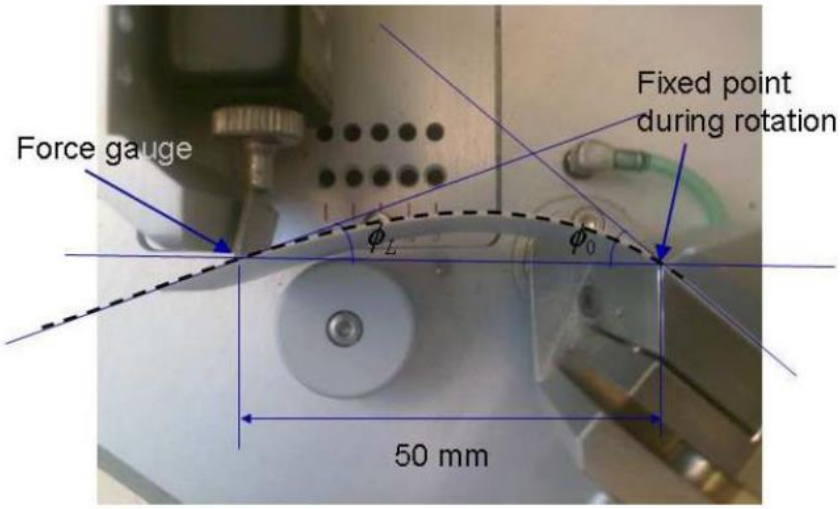

Fig. 9: In plane bending test

The FE simulations are done using fully integrated shell elements and *MAT_PAPER with one ply, see Fig. 10. The element size is 1x1 mm and the width of the test specimen is 38 mm. Three different lengths were simulated (10 mm, 25 mm and 50 mm) in both CD and MD directions, and the results were compared with experiments. The simulations captures the overall paperboard behavior such as initial stiffness and maximum torque, see Fig. 11.

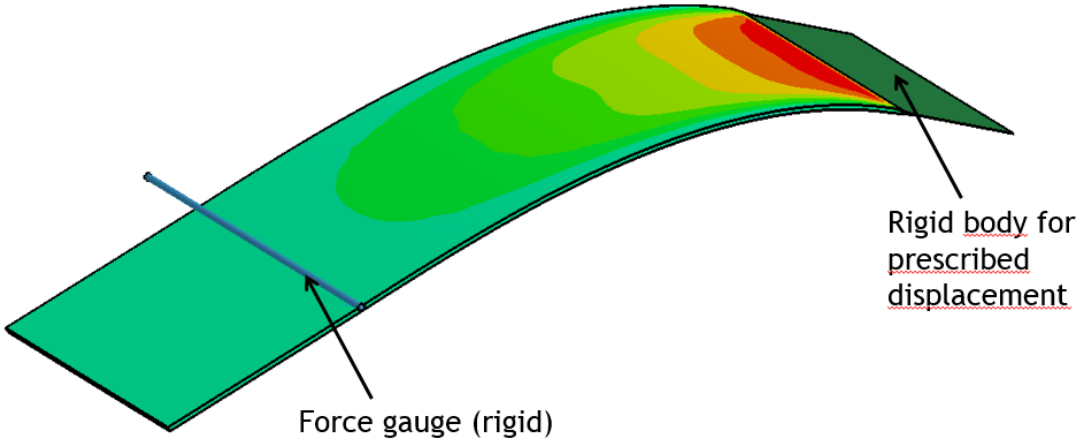

Fig. 10: Finite element model of in plane bending test

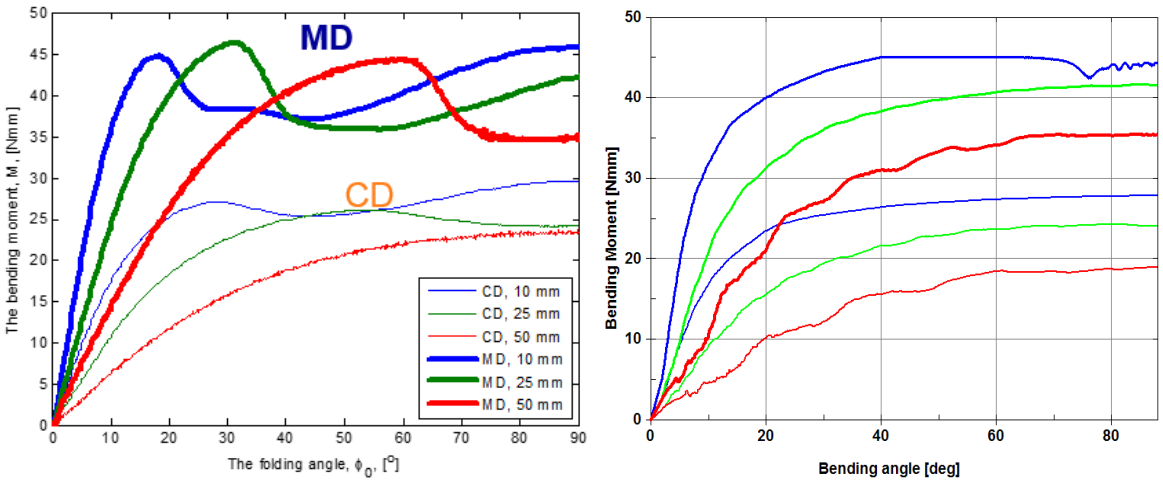

Fig. 11: Bending torque versus angle for different paperboard lengths and directions, test (left) and simulation (right)

5.2 Creasing

To verify the out of plane modeling, the creasing experiments according to Nygårds et al. [10] was simulated. The experiments are done with two different creasing depths; 0 mm and 0.2 mm. This corresponds to when the punch is at the die level and 0.2 mm below. The FE model consists of fully integrated hex elements with one element in the width direction to save computational time. Single point constraints were applied to mimic a plane strain condition. The paperboard is built up by 3 plies and cohesive elements were used between the different plies to model delamination, see Fig. 12. The paperboard is pre-tensioned in the MD direction before creasing. The simulated creasing deformation is shown in Fig. 13, and the crease force comparison is shown in Fig. 14. The simulations show good agreement with experiments.

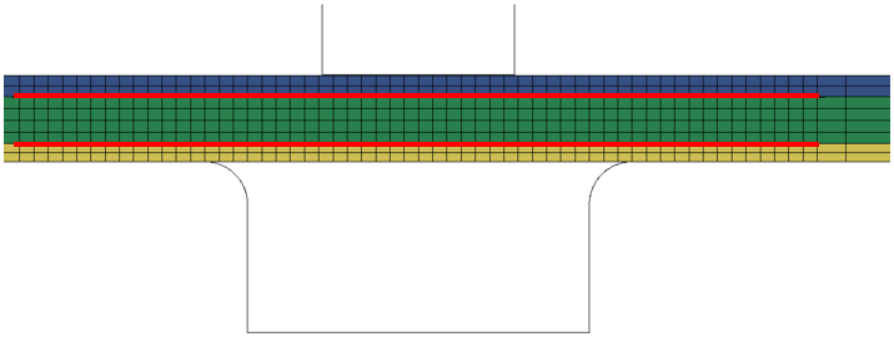

Fig. 12: Finite element model of creasing tool. The cohesive elements are marked as red.

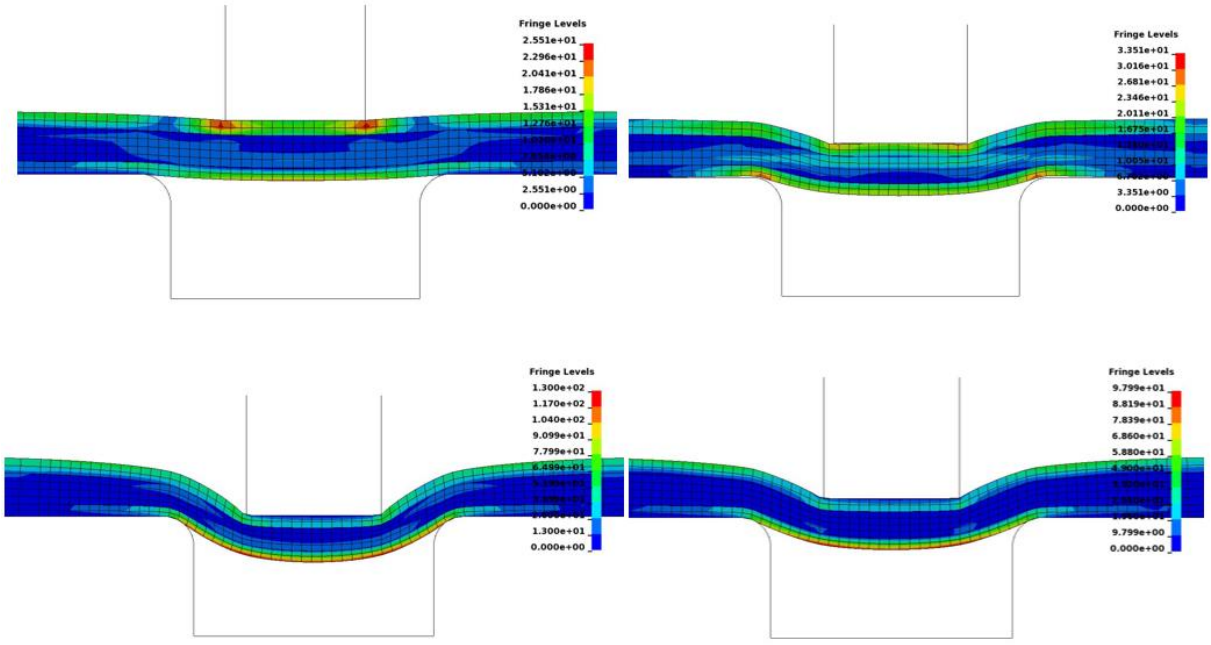

Fig. 13: Simulated creasing deformation for a 0. mm crease depth.

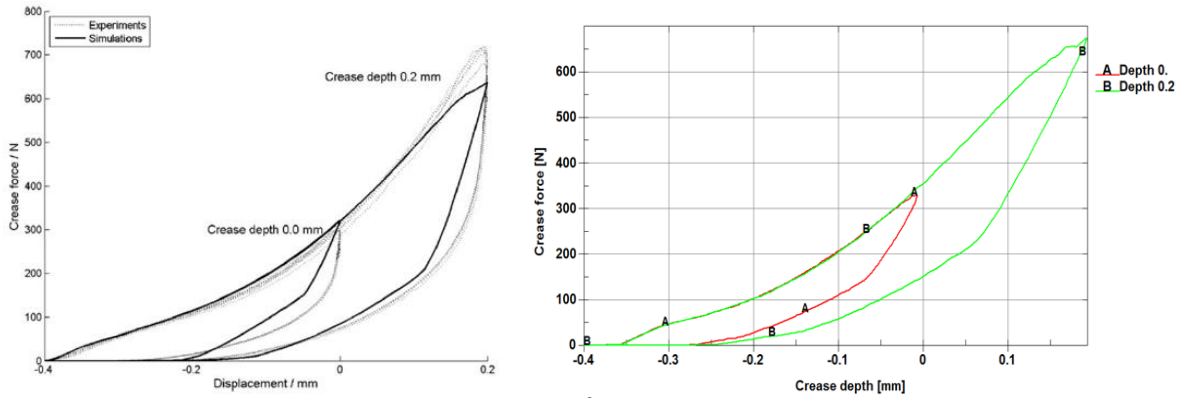

Fig. 14: Crease forces from experiments (left) from Nygårds et al. [10] and simulation (right).

6 Summary

Paperboard is a highly anisotropic material due to the production process where the fibers align in the MD direction orthogonal to the CD direction where the properties are several times lower. Further, the properties in the thickness direction (ZD) are significantly less compared to the MD direction. To accommodate for this, the material model according to Xia [9] and Nygårds et al. [10] have been implemented in to LS-DYNA. The material model consists of an in plane yield surface that are built up by 6 yield planes, a through thickness compression yield surface and an out of plane shear yield surface. The model is implemented in a solid and a shell version. The shell version can be used to model the bending stiffness of the paperboard, and combined with ***PART_COMPOSITE,** several plies can be combined to create a layered multi-ply board. In out of plane deformation, paperboard is likely to experience delamination. This is typically modeled using cohesive layers between rows of solid elements. The implementation and modeling techniques have been verified in a bending test and a creasing test. The simulations shows good agreement with the experiments.

7 Literature

[1] Dunn, H.: “Micromechanics of paperboard deformation”, Master’s thesis, Massachusetts Institute of Technology, 2000
[2] Nagasawa, S., Endo, R., Fukuzawa, Y.,Uchino, S. and Katayama, I.: “Creasing characteristic of aluminium coated paperboard”, Journal of Materials Processing Technology, 201(1-3), 2000 , 401-407
[3] Borgqvist, E.: “Continuum modeling of the mechanical properties of paperboard”, Licentiate Dissertation, Lund University, 2014
[4] Tryding, J.: “In plane fracture of paper”, PhD Thesis, Lund Institute of Technology, 1996
[5] Mäkelä, P., Östlund, S.:”Orthotropic elastic-plastic material model for paper materials”, International Journal of Solids and Structures, 40 (21), 2003, 5599-5620
[6] Nygårds, M.: “Experimental techniques for characterization of elastic-plastic material properties in paperboard”, Nordic Pulp and Paper Research Journal, 23 (4), 2008, 432-437
[7] Lindström, T.: “In-plane paperboard model”, Master’s Thesis, Lund Institute of Technology, 2013
[8] Stenberg, N.: “On the Out-of-Plane Mechanical Behaviour of Paper Materials”, PhD Thesis, Royal Institute of Technology, Stockholm, 2002
[9] Xia, Q. S.: “Mechanics of inelastic deformation and delamination in paperboard”, PhD Thesis, Massachusetts Institute of Technology, 2002
[10] Nygårds, M., Just, M. and Tryding, J.: “Experimental and numerical studies of creasing of paperboard”, International Journal of Solids and Structures, 46, 2009, 2493-2505